Acta Sci. Pol.
Architectura 20 (1) 2021, 51–64
content.sciendo.com/aspa ISSN 1644-0633 eISSN 2544-1760 DOI: 10.22630/ASPA.2021.20.1.6

ORIGINAL PAPER

Received: 28.12.2020
Accepted: 16.02.2021

STRENGTH AND STABILITY OF STRUCTURES WITH NODES FLEXIBLE IN TERMS OF SHIFT

Jan Zamorowski✉

Faculty of Materials, Civil and Environmental Engineering, University of Bielsko-Biala, Bielsko-Biała, Poland

ABSTRACT

Distribution of internal forces in bar structures in relation to rotational flexibility of their nodes is widely discussed in the literature. However, the investigations concerning such structures with nodes flexible in terms of shift are less frequent. This paper presents examples of structures, in which the shift flexibility of lap joints determined their load-bearing capacity and stability, as well as the serviceability limit states. A low-rise dome, a covering of the exhibition hall in Chorzów, which collapsed in 2006, and a mobile telephony tower were depicted. Mechanical models describing rotational stiffness and shift flexibility of various lap joints by means of component method were used. Mathematical model by Kishi and Chen was applied to model the susceptibility of lap joints under alternating loads. In case of the low-rise dome, the results indicated that the failure was determined by joint clearances. In case of covering of the exhibition hall in Chorzów, flexibility of joints resulted in excessive utilization of resistance in certain lattice purlins, which could have initiated the disaster. In turn, flexibility of connections rarely considered in the design of mobile phone towers may result in an excessive sway of the tower legs on which the antennas of the radio link are suspended and thus interfere transmitted signals. The study showed that there is a need to take into account the influence of flexible nodes, not only in the structures sensible to deformations like low-rise domes, but also in the other structures, like mobile phone towers, in which their serviceability limit state is decisive.

Key words: nodes flexibility in terms of shift, flexibility lap joints in terms of shift and rotation, modelling of structures with nodes flexible in terms of shift

INTRODUCTION

The stiffness and the resistance of the nodes in I-section members connections are checked according to Point 6 in the standard EN 1993-1-8 (European Committee for Standardization [CEN], 2005). Meanwhile, modelling of structures with nodes flexible in terms of shift is less widely known. There is a lack of rules for the classification of such joints as well as formulas for their stiffness calculation in the standard EN 1993-1-8.

In the general case, in the analysis of bar structures with nodes flexible in terms of shift, physical models based on test results, mathematical models with coefficients calibrated on the basis of test results as well as mechanical models may be used. The test results carried on lap joints published in the literature mainly concern thin-walled components connected with blind fasteners the BOM type (Wuwer, 2006; Zamorowski, Świerczyna & Wuwer, 2011), which were tested for both monotonic and alternating loads. Studies on bolted lap joints are less frequently published. There is a lack of catalogued test results for typical snug-tight and prestressed lap joints (Karczewski, Wierzbicki & Witkowski, 2003), from which N–δ curves could be directly obtained, both for monotonic and alternating loads.

Jan Zamorowski https://orcid.org/0000-0003-4394-4821
✉JZamorowski@ath.bielsko.pl

This paper presents mechanical models for various bolted lap joints based on the component method provided by the standard EN 1993-1-8 for beam-to-column joints. These models allow to describe fairly well both the behavior of axially loaded and twisting moment-loaded joints. The presented mechanical models were used to analytically investigate the behavior of the nodes of the broke down low rise dome and covering of the exhibition hall in Chorzów that collapsed in 2006.

In case of alternating loads, however, these models are useless, because the N–δ dependence at such loads is arranged in the form of a hysteresis loop, which is easiest to describe by mathematical models. The coefficients in these models are calibrated on the basis of the experimental tests results. Numerical studies were carried out by use the model of Kishi and Chen (1990). Coefficients applied in this model were estimated based on the results of Karczewski et al. (2003) and Wuwer (2006). Wuwer tested lap joints with hole-filling BOM fasteners under alternating loads, while Karczewski et al. tested pre-stressed and non-pre-stressed high-strength bolted connections under monotonic loads. Tests on connections with non-preloaded bolts revealed a slippage due to clearances determined by the diameter of the bolt adopted and the hole executed. Taking these results, it was possible to estimate the course of the hysteresis loop for lap connections which are applied in mobile phone towers. An example tower with a height of 50.4 m was examined.

The results of numerical investigations of bar structures with nodes flexible in terms of shift presented in this paper indicate that in such structures, due to clearances in connections or flexibility of connections, pre-failure states or even to construction disasters, or operational difficulties may occur.

BASES OF CALCULATIONS

A pre-bent, hinged-hinged bar, flexibly shift-joined, loaded at the ends with axial force, lateral load and moments is considered (Fig. 1).

It is assumed that the shortening of the bar chord Δl_k in any incremental step is the sum of the shortenings: from the impact of the increase in axial force $\Delta l\varepsilon_k$, the change in curvature $\Delta l\kappa_k$, and the effect of flexible nodes in the initial node $\Delta l_{\delta k,\bar{p}}$ and in the end node $\Delta l_{\delta k,\bar{k}}$. The substitute axial stiffness of the bar with this assumption can be expressed in the following formula

$$(EA)_z = \frac{\Delta N_k \cdot l_0}{\Delta l_k} = \frac{\Delta N_k \cdot l_0}{\Delta l_{\varepsilon k} + \Delta l_{\kappa k} + \Delta l_{\delta k,\bar{p}} + \Delta l_{\delta k,\bar{k}}} \quad (1)$$

where $\Delta l_{\varepsilon k} = \Delta N_k \cdot l_0 / EA$, and l_0 is initial length of the bar.

Using the approximate formula for the difference in the length of the curve and its chord, the increase in bar chord shortening due to a change in curvature, in k-th step is calculated from the following formula

$$\Delta l_{\kappa k} = \frac{\pi^2}{4l_0} \sum_n n^2 f_{kn} \left(f_{kn} + 2 f_{0n} + 2 \sum_{m=1}^{m=k-1} f_{mn} \right) \quad (2)$$

where:

f_{kn}, (f_{mn}) – n – the amplitude of k, (m) increase in elastic bend, which can be determined according to the formulas presented by Zamorowski (2013),

f_{0n} – n-th amplitude of the initial deformation of the bar.

The increase in bar shortening from the impact of a flexible connection at one end is determined by the following formula

$$\Delta l_{\delta k} = \frac{N_k}{K_{\delta k}} - \frac{N_{k-1}}{K_{\delta k-1}} \quad (3)$$

in which $K_{\delta k}$ and $K_{\delta k-1}$ are secant stiffness of the connection in k-th and $k-1$ incremental step.

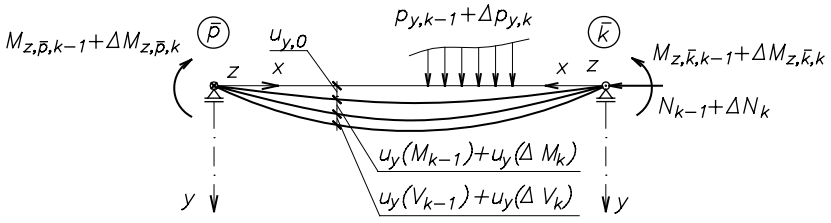

Fig. 1. The bar scheme

The results of studies of lap joints available in the literature describe mainly the relations between force and shift (N–δ) with increasing value of force (Karczewski et al., 2003). However, there are few results of such tests at alternating loads. They indicate, however, that the N–δ relation (similarly to M–φ) at alternating loads, is arranged in the form of a hysteresis loop with a larger or smaller narrowing (Wuwer, 2006), where the results of tests of lap joints with BOM R16 pins are presented (Fig. 2).

The changes in the N–δ relation can be predicted with the same functions as for the changes in the M–φ relation in bent joints (Fig. 3).

Curve I at the first load and when the load increases over the load from previous steps, and Curve III after the first change of direction of the load in the joint and with the increase of this load can be described by the functions of Kishi and Chen (1990) as for bent lap joints – see functions in Formula (4). Lines II and IV, in turn, are parallel to the

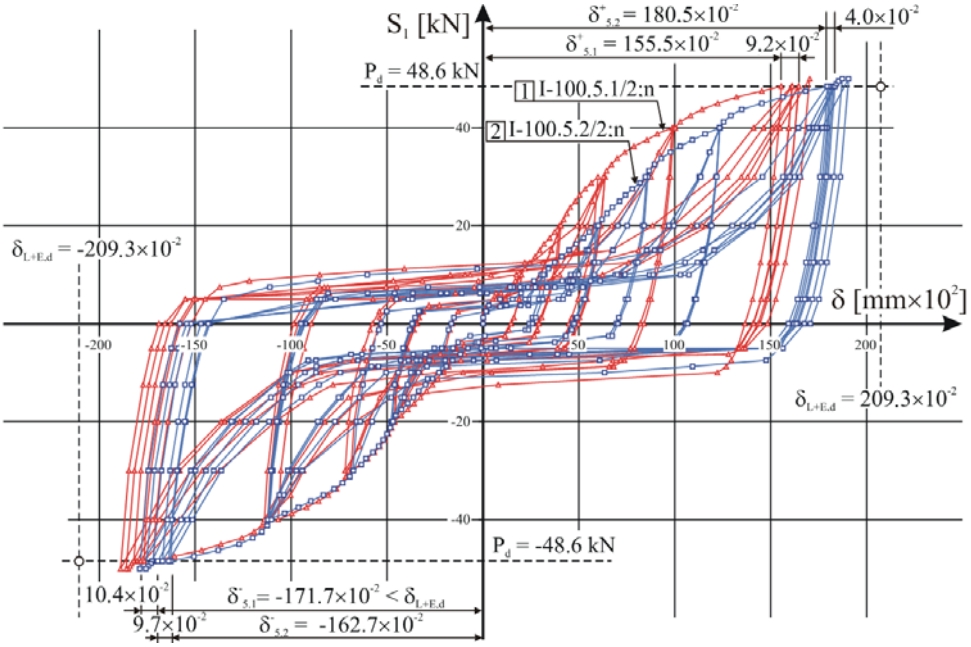

Fig. 2. S_1–δ charts for alternately loaded joints with BOM R16 pins (Wuwer, 2006)

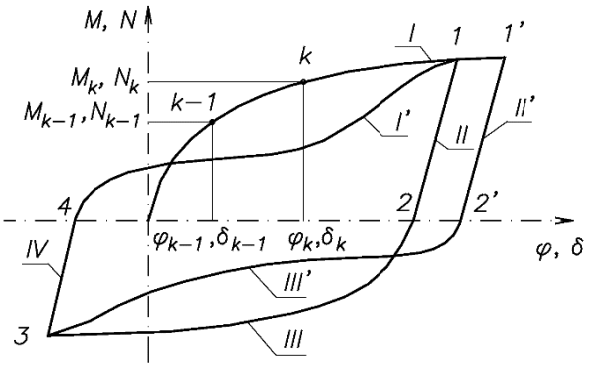

Fig. 3. The M–φ and N–δ relation in the case of alternating loads

tangents to Curves I and III in Points 0 and 2 respectively. Curves I' and III' are described by functions in Formula (5).

$$N_{\mathrm{I}} = \frac{K_{ri,\mathrm{I}} \cdot \delta}{\left[1+\left(\frac{\delta}{\delta_{0\mathrm{I}}}\right)^{c_{\mathrm{I}}}\right]^{\frac{1}{c_{\mathrm{I}}}}}$$

$$N_{\mathrm{III}} = \frac{K_{ri,\mathrm{III}} \cdot (\delta - \delta_2)}{\left[1+\left(\frac{|\delta - \delta_2|}{\delta_{0\mathrm{III}}}\right)^{c_{\mathrm{III}}}\right]^{\frac{1}{c_{\mathrm{III}}}}} \tag{4}$$

$$N_{\text{I}'} = \frac{N_1}{\delta_1 - \delta_4}(\delta - \delta_4) + a_{\text{I}'} N_1 \sin\frac{3\pi(\delta - \delta_4)}{\delta_1 - \delta_4} - b_{\text{I}'} N_1 \sin\frac{\pi(\delta - \delta_4)}{\delta_1 - \delta_4}$$
$$N_{\text{III}'} = -\frac{N_3}{\delta_{2'} - \delta_3}(\delta - \delta_{2'}) - a_{\text{III}'} N_3 \sin\frac{3\pi(\delta - \delta_{2'})}{\delta_{2'} - \delta_3} + b_{\text{III}'} N_3 \sin\frac{\pi(\delta - \delta_{2'})}{\delta_{2'} - \delta_3} \tag{5}$$

The coefficients in these formulas can be estimated on the basis of the results of lap joint tests.

For increasing loads, the rigidity of lap joints can be estimated quite well using formulas based on the component method (Table 1).

The rigidity components of a single bolt in Table 1 are calculated from the following formulas

$$k_{11} = \frac{8d^2 f_{ub}}{d_{M16}}, \quad k_{12} = 12 k_b k_t d f_u \tag{6}$$

Table 1. Stiffness of lap joints (Zamorowski et al., 2011)

No	Lap joints	Joint rigidity
1	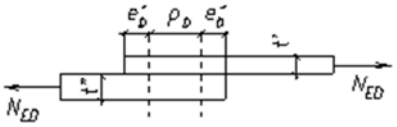	$K_\delta = \frac{1}{\frac{1}{nk_{11}} + \frac{1}{nk_{12}'} + \frac{1}{nk_{12}''}}$
2	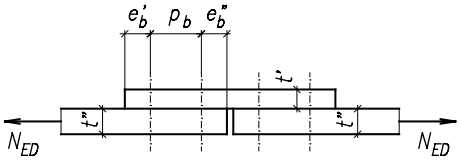	$K_\delta = \frac{1}{\frac{2}{nk_{12}''} + \frac{2}{nk_{12}'} + \frac{2}{nk_{11}}}$
3	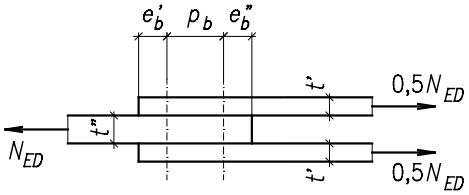	$K_\delta = \frac{1}{\frac{1}{nk_{12}''} + \frac{1}{2nk_{12}'} + \frac{1}{2nk_{11}}}$
4	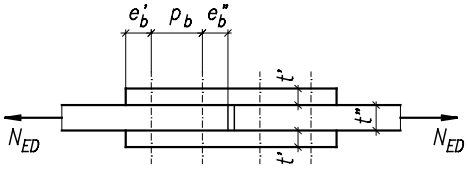	$K_\delta = \frac{1}{\frac{2}{nk_{12}''} + \frac{2}{2nk_{12}'} + \frac{2}{2nk_{11}}}$
5	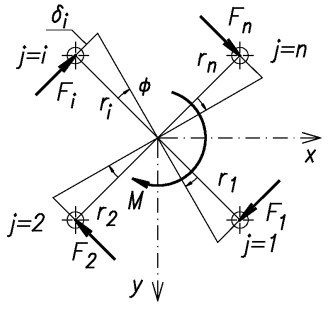	where $K_{\delta i}$ – like $K_\phi = K_{\delta i}\sum_{j=1}^{n} r_j^2$, according to Item (1) or (3) for $n = 1$.

in which

$$k_b = \min\begin{Bmatrix} 0.25\,e_b/d + 0.5 \\ 0.25\,p_b/d + 0.375 \\ 1.25 \end{Bmatrix},\ k_t = \min\begin{Bmatrix} 1.5\,t_j/d_{M16} \\ 2.5 \end{Bmatrix}$$

and other designations according to Table 6.11 in the standard EN 1993-1-8.

The results obtained from Formula (6) presented above reflect the actual rigidity of such joints quite well (Zamorowski et al., 2011).

EXAMPLES OF CALCULATIONS

Three examples of completed structures were presented, in which the flexibility of the lap joints in terms of shift was decisive or could determine the bearing capacity, stability or conditions of use. In the two examples N–δ relations, estimated according to the formulas specified in Table 1, were used. In the third example, the behaviour of structures under alternating loads was analysed.

Example 1 – a low-rise dome

The domes with the shape of a spherical bowl and a height of 5 m covered the exhibition pavilions, in a circular section view with a diameter of 30 m (Fig. 4a). They were made as bar grids with triangular meshes of triangle side lengths varying from 1.091 to 1.026 mm. Bars made of 33 × 3.5 mm diameter pipes were linked in nodes to 8 mm thick gusset plates. At each node, three bars were welded to the gusset plate, and three were connected to this plate using M10 bolts, with a thread along the entire length (Fig. 4b).

The failure of the domes took place after several years of use of the pavilions. The first dome collapsed at night after blowing snow from its windward part to its leeward part. The second dome failed during the next day while snow was being removed from it. After the failure, it was found that the outer thread diameter of the bolts in the links was between 9.5 and 9.7 mm, and the bolt holes in the gusset plates were 12 mm in diameter instead of 11 mm (Augustyn & Śledziewski, 1976).

Joint rigidity was estimated for the following data: d = 9.6 mm, f_{ub} = 400 MPa, f_u = 360 MPa, e_b = 20 mm, p_b = 35 mm, t' = t'' = 8 mm.

Using Formula (1) in Table 1 for n = 2, K_δ = 21.73 kN·mm^{-1} was obtained.

The calculations took into account the dead load of the steel structure, the cover and two snow load cases (Fig. 5).

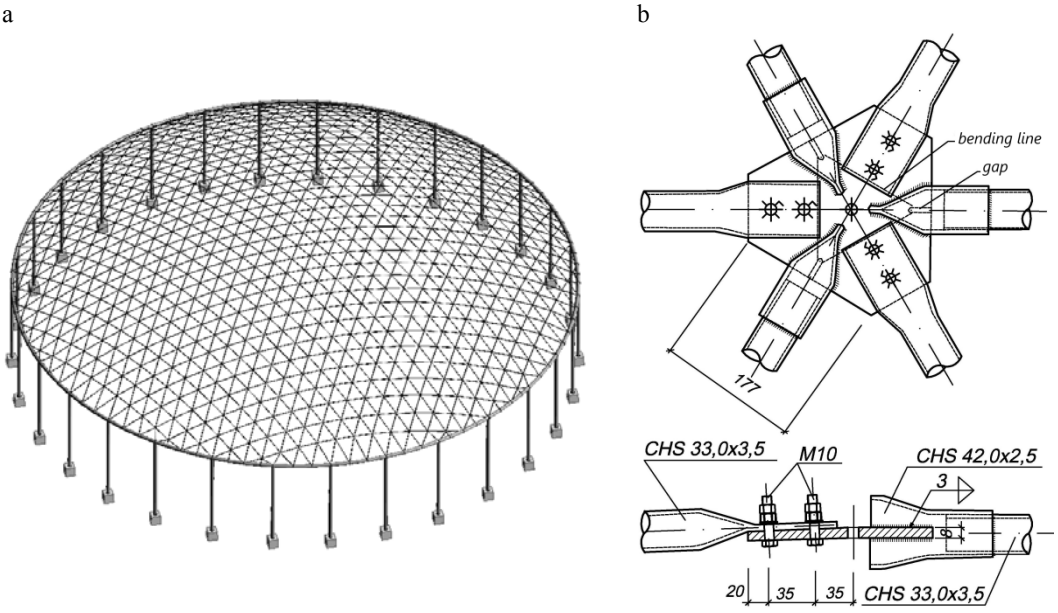

Fig. 4. Bar dome: a – calculation model; b – mesh node

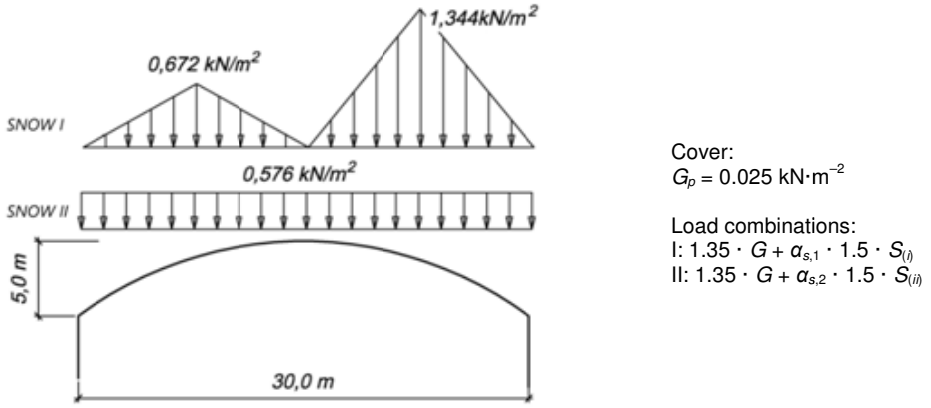

Fig. 5. Dome load

In the dome stability analysis, the value of the α_s coefficient (Fig. 5) at which the dome lost its stability was sought. The obtained results are summarized in Table 2.

Values above 1.0 in Table 2 mean that under normal snow loads the dome should not lose stability. The dome failure occurred at an asymmetrical snow load, closer to Scheme II (Snow II) with a maximum value of approximately 50% of the normal snow load. This means that the cause of the disaster were loose joints. The maximum possible slip in the joint was δ = 12 – 9.6 = 2.4 mm. The dome geometry, in turn, was arranged in such a way that the difference between the length of the bar and its projection on the plane determined by the adjacent nodes was only 0.25 mm. Thus, after overcoming the friction forces, there could be a local shift of the middle node to the inside of the hexagon plane.

Table 2. Values of coefficients $\alpha_{s,1}$ and $\alpha_{s,2}$

No	Type of analysis	No local imperfections		With local imperfections	
		$\alpha_{s,1}$	$\alpha_{s,2}$	$\alpha_{s,1}$	$\alpha_{s,2}$
1	Rigid nodes	4.00	2.93	3.27	2.41
2	Flexible nodes without slip	1.79	1.12	1.64	1.04
3	Flexible nodes with slip	0.54	0.51	0.50	0.47

Example 2 – the covering of the collapsed exhibition hall in Chorzów

In the construction design of the exhibition pavilion at the International Katowice Trade Fair, which collapsed in January 2006, the roof slope segments were designed as structures (Fig. 6) supported on lattice binding joists, external columns (rockers of curtain walls) and one or two main hall columns. In the completed structure, the bars connecting the top nodes of the structure in a direction parallel to the axes A and B were abandoned (see dashed line in Fig. 6). As a result, the structure consisted of vertical trusses shown in Figure 6 in odd axes and diagonal trusses with common upper chords for two trusses in even axes and lower chords common for vertical trusses.

In both types of trusses – vertical and oblique ones, the N-type truss was used. The truss chords were made of 100 × 100 × 4 mm square-section pipes, while the cross-braces, and elements connecting the lower structure nodes in a direction parallel to axes A and B of 50 × 50 × 4 mm pipes. The dimensions of the analysed roofing structure were 24.8 × 24.0 m, and its height was 2.4 m. All nodes except the support shoes and cross-braces joints of diagonal trusses with chords were welded.

The cross braces in the diagonal trusses were connected to the chords using M20-4.6 bolts (f_{ub} = 400 MPa) using 6 mm thick gusset plates (f_u = 360 MPa) – see Figure 7.

Various solutions were used for the joints, including: oval holes located in a direction perpendicular to

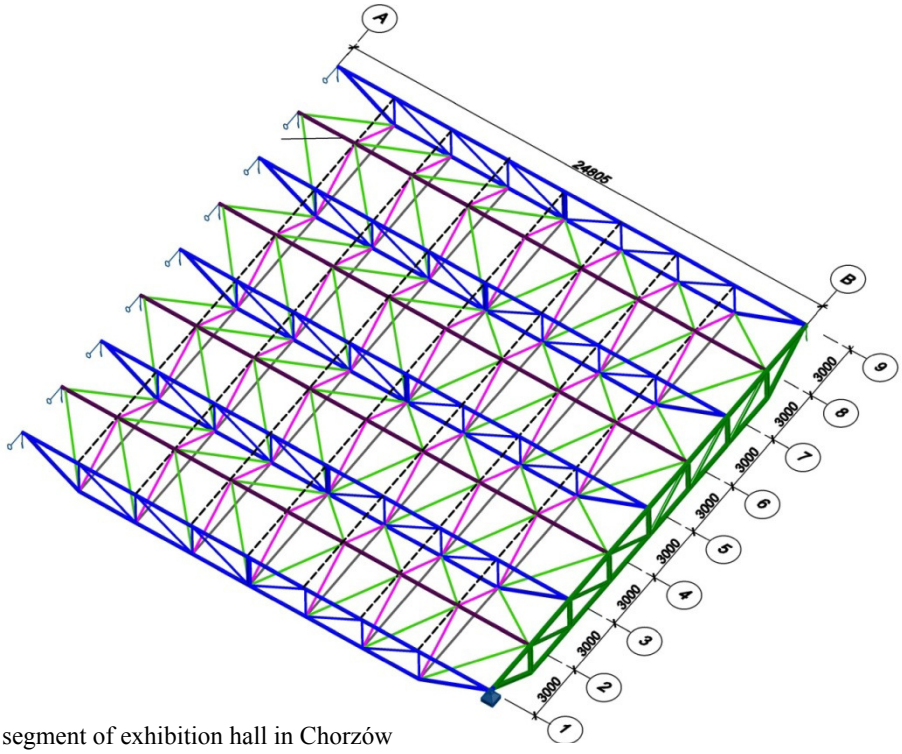

Fig. 6. Roof segment of exhibition hall in Chorzów

the bar axes (Fig. 7a), one bolt placed in the oval hole (Fig. 7b), two bolts located in the oval holes parallel to the bar axis or by means of an additional plate with an oval hole also parallel to the bar axis.

Various systems were analysed: with rigid nodes, with double bolts at both ends of cross-braces in oblique trusses, with single bolts in these nodes and a system without cross-braces in oblique trusses. Joint rigidity was estimated using the component method as for normal holes. For oval holes, this rigidity was reduced by a factor of 0.6, which is used in the standard EN 1993-1-8 when determining the load capacity of such bolts. The possibility of slip between sheets in the joints was also taken into account, assuming the value of 2 mm at one end of the bar in the oval hole perpendicular to the bar axis, and 8 mm in the hole

a b

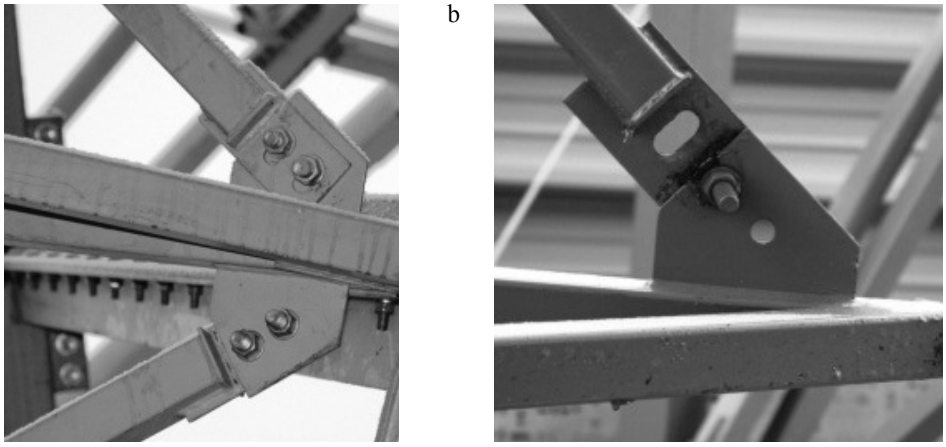

Fig. 7. Joints of angle braces with lower vertical truss chords: a – with oval holes; b – with only one bolt

parallel to the axis. It was assumed that the slip can occur at a force (F) corresponding to a friction force at a bolt compression of 25% of the maximum compression force.

The slip rigidity of the joint was obtained from Formula (1) in Table 1. Taking into account the nominal characteristics of the connection with round holes: $d = 16$ mm, $d_o = 18$ mm, $e_b = 25$ mm, $p_b = 40$ mm, $t' = t'' = 6$ mm and $f_{ub} = 400$ MPa, $f_u = 360$ MPa, the following results were obtained: $k_{11} = 51.2$ kN·mm^{-1}, $k_b = 0.891$, $k_t' = k_t'' = 0.563$, $k_{12}' = k_{12}'' = 34.67$ kN·mm^{-1}, and in addition: with two bolts in joint $K_\delta = 25.90$ kN·mm^{-1}, for one-bolt joint $K_\delta = 12.95$ kN·mm^{-1}.

After reduction of the rigidity of joints with oval holes by a factor of 0.6 the following results were obtained: for two bolts in the joint $K_\delta = 15.54$ kN·mm^{-1} and for one bolt $K_\delta = 7.77$ kN·mm^{-1}.

The obtained results for selected roof covering elements, with a load of the cover of $g_k = 0.20$ kN·m^{-2} and a snow load of $s_k = 0.72$ kN·m^{-2}, are presented in Tables 3 and 4 for connections with two bolts and one bolt, respectively.

Table 3. Axial forces in truss elements in Axis 5 and its deflection with a joint of two bolts

No	Element		Nodes of angle braces					No angle braces
			rigid nodes	normal hole	oval holes			
					perpendicular	perpendicular with slip	parallel with slip	
1	No local arch imperfections							
	Upper chord	[kN]	159.5	191.9	203.9	225.3	265.9	281.9
		[%]	100	120.3	127.8	141.2	166.7	176.8
	Bottom chord	[kN]	–277.7	–273.4	–271.1	–269.9	–267.7	–262.7
		[%]	100	98.5	97.6	97.2	96.4	94.6
	Support cross brace	[kN]	–105.3	–116.1	–123.1	–130.9	–158.0	–159.9
		[%]	100	110.3	116.9	124.4	150.1	151.9
	Deflection	[mm]	83.7	87.3	89.3	93.3	101.4	104.1
		[%]	100	104.3	106.7	111.5	121.2	124.4
2	Including local arch imperfections $e_0 = l/200$							
	Upper chord	[kN]	162.3	191.5	205.5	223.1	263.9	282.3
		[%][a]	101.8	120.1	128.8	139.9	165.5	177.0
		[%][b]	101.8	99.8	100.8	99.0	99.3	100.1
	Bottom chord	[kN]	–279.4	–277.4	–278.6	–274.4	–270.2	–263.8
		[%][a]	100.6	99.9	100.3	98.8	97.3	95.0
		[%][b]	100.6	101.5	102.8	101.7	100.9	100.4
	Support cross brace	[kN]	–94.4	–116.3	–125.1	–130.6	–160.0	–161.7
		[%][a]	89.7	110.4	118.8	124.0	151.9	153.6
		[%][b]	89.7	100.1	101.7	99.7	101.3	101.1
	Deflection	[mm]	87.1	93.5	97.1	100.4	110.4	114.9
		[%][a]	104.1	111.7	116.0	119.9	131.9	137.3
		[%][b]	104.1	107.1	108.7	107.6	108.9	110.4

[a] Referred to rigid nodes without imperfections; [b] referred to rigid nodes with imperfections.

Table 4. Axial forces in truss elements in Axis 5 and its deflection with a joint of one bolt

No	Element		Nodes of angle braces				
			rigid nodes	normal hole	oval holes		
					perpendicular	perpendicular with slip	parallel with slip
1	No local arch imperfections						
	Upper chord	[kN]	159.5	210	224.8	240.9	271.8
		[%]	100	132.0	140.9	151.1	170.4
	Bottom chord	[kN]	–277.7	–272.7	–270.5	–269.3	–267.5
		[%]	100	98.2	97.4	97.0	96.3
	Support cross brace	[kN]	–105.3	–128.0	–135.2	–140.8	–160.0
		[%]	100	121.5	128.4	133.7	152.0
	Deflection	[mm]	83.7	91.0	93.5	96.4	102.5
		[%]	100	108.7	111.7	115.2	122.5
2	Including local arch imperfections $e_0 = l/200$						
	Upper chord	[kN]	162.3	211.1	224.4	238.7	270.0
		[%][a]	101.8	132.3	140.7	149.6	169.3
		[%][b]	101.8	100.3	99.8	99.1	99.3
	Bottom chord	[kN]	–279.4	–279.0	–275.6	–273.2	–270.3
		[%][a]	100.6	100.5	99.3	98.4	97.3
		[%][b]	100.6	102.3	101.9	101.4	101.0
	Support cross brace	[kN]	–94.4	–128.6	–136.4	–140.9	–161.3
		[%][a]	89.7	122.1	129.5	133.8	153.2
		[%][b]	89.7	100.5	100.9	100.1	100.8
	Deflection	[mm]	87.1	98.6	101.3	104.1	111.8
		[%][a]	104.1	117.8	121.0	124.4	133.6
		[%][b]	104.1	108.9	108.3	108.0	109.1

[a] Referred to rigid nodes without imperfections; [b] referred to rigid nodes with imperfections.

In the case of cross-bracing in diagonal trusses with two screws placed in the normal round holes, forces in the upper truss chord in Axis 5 will increase by approximately 20% when compared to the forces in the truss with rigid nodes, and by 10% in the support cross-braces of this truss. If, however, the rigidity of the joints of these cross-braces is assumed to be as for an oval hole in the direction perpendicular to the axis of the bar, with slip (as in the case of most nodes in the collapsed object), then the values of axial forces increase by 41% in the upper chords, and by 24% in the cross-braces. For flexibility of joints as for oval holes along the bar axis and the joint rigidity with slip, there is be an increase in forces by 66.7% in the upper chord and by 50% in the cross-brace. These values are only slightly lower than in the roof structure without cross-bracing in diagonal trusses, for which the values of 76.8% and 52%, respectively, were obtained. Deflection in all of the above cases increased by 4.3%, 11.5%, and 21.2%, respectively.

The inclusion of local bow imperfections in compressed bars in structures with flexible nodes practically no longer affects the distribution of internal forces. The deflection of such a structure, however, increases up to 9% as compared to the deflection calculated without bow imperfections.

In the case of cross-braces joints with one bolt, the increase in the value of forces in the upper chord and the cross-brace is slightly larger and amounts to: 32% and 21.5% for normal round holes, 51% and 33.7% for oval holes perpendicular to the bar axis and 70.4% and 52% when the oval holes are located in a direction parallel to the axis of the rod, respectively. The deflection of the truss with flexible nodes and local imperfections will increase for the cases presented above in relation to the truss with rigid nodes by 17.8%, 24.4% and 33.6%, respectively. The obtained results indicate that the behaviour of the roof with the cross-bracing joints in oblique trusses as in Figure 7a and b is closer to the behaviour of structures without cross braces in diagonal trusses than to structures with rigid nodes.

Example 3 – mobile telephony tower

A steel mobile telephony tower with a square cross section, a height of 50.4 m and geometrical characteristics of the wall as in Figure 8a was analysed. It was assumed that the bars are rigidly connected in the nodes and the tower support is articulated. The calculations took into account the flexibility of lap joints of columns with the design as in Figure 8b, arranged at the height of the wall in accordance with the dimensions as in Figure 8a. Five M16 bolts in one angle leg were adopted for the joints.

The truss was loaded with its own weight and periodically with wind load. Each wind load cycle was divided into four phases. In the first phase of the first cycle, the increase in forces and displacements for the wind load on the left side of the lattice was added to

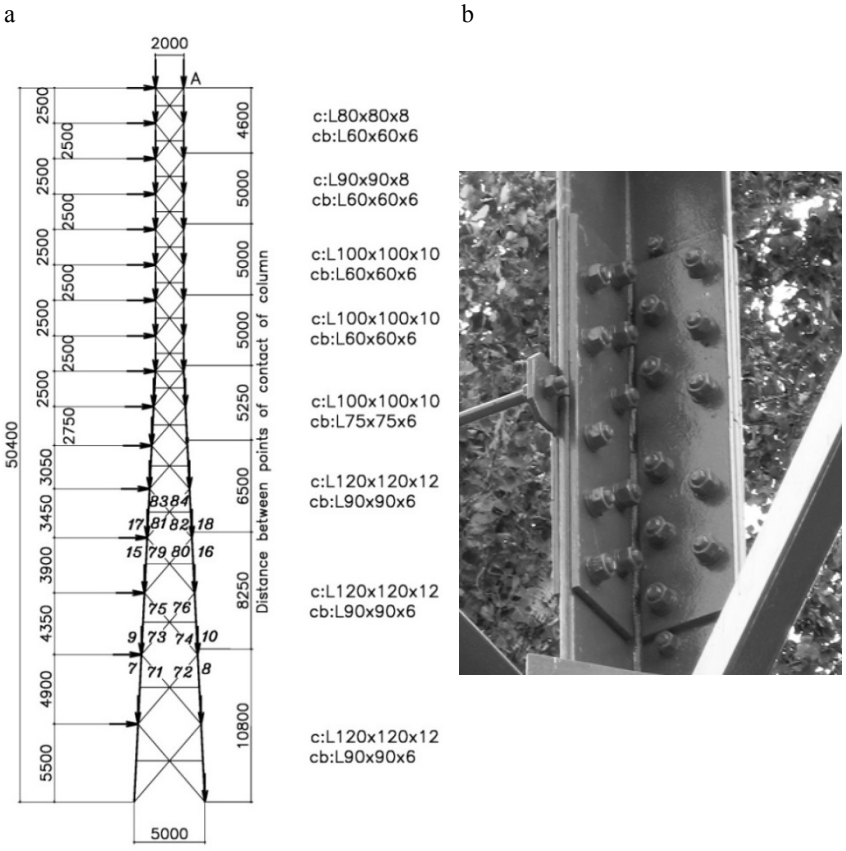

Fig. 8. Analysed tower: a – characteristics of the tower wall; b – overlap joint

the sum of the increases in forces and displacements obtained for the own weight load. In the second phase, a relief took place. In the next steps, the increases of forces and displacements for wind load were added to the previous sums, as in the first phase, but with the opposite sign. In the third phase, the lattice was loaded with wind acting from the right side, and in the fourth phase, the load was relieved again. After each cycle the system was loaded only by its own weight. The last load cycle was limited to the first phase.

In subsequent cycles and load phases, the flexibility characteristics of joints changed in accordance with N–δ hysteresis loop presented in Figure 3 with the equations of branches in Formulas (4) and (5). Using the results by Wuwer (2006) and Karczewski et al. (2003), which related to slightly different joints, the values of the coefficients in Formulas (4) and (5) were estimated.

The basis for calibrating these coefficients was their compression load-bearing capacity. The following values were assumed: $K_{ri,\mathrm{I}} = 400$ MN·m^{-1}, $K_{ri,\mathrm{III}} = 360$ MN·m^{-1}, $\delta_{0\mathrm{I}} = \delta_{0\mathrm{III}} = 0.006$ m, $c_{\mathrm{I}} = c_{\mathrm{III}} = 0.5$, $a_{\mathrm{I}'} = a_{\mathrm{III}'} = 1/30$, $b_{\mathrm{I}'} = b_{\mathrm{III}'} = 1/15$. In the calculations, the effect of initial bar bending was disregarded. The values of axial forces obtained in selected truss bars (in the area of the two lower contact points) are presented in Table 5, and the displacement values $u(u_x, u_y, \phi)$ of the node A, in Table 6.

Column 3 of Table 5 presents the values of forces obtained in the solution without affecting the flexibility of the joints, assuming the initial bar deflections are $f_0 = 0$.

Table 5. Values of axial forces in selected truss bars (acc. to Fig. 8)

Position	Force	No flexible nodes	With flexible nodes					
			Cycle 1 Phase 1		Cycle 2 Phase 1		Cycle 5 Phase 1	
		F [kN]	F [kN]	$\frac{(4)-(3)}{(3)}100$	F [kN]	$\frac{(6)-(3)}{(3)}100$	F [kN]	$\frac{(8)-(3)}{(3)}100$
1	*2*	*3*	*4*	*5*	*6*	*7*	*8*	*9*
Columns	F_7	–148.64	–148.76	0.1	–149.99	0.9	–150.08	1.0
	F_8	178.16	178.24	0.0	177.09	–0.6	176.96	–0.7
	F_9	–134.81	–134.75	0.0	–133.26	–1.1	–133.03	–1.3
	F_{10}	159.44	159.42	0.0	160.92	0.9	161.06	1.0
Cross-braces	F_{71}	12.08	12.02	–0.5	13.59	12.5	13.72	13.6
	F_{72}	–9.88	–9.78	–1.0	–8.21	–16.9	–8.06	–18.4
	F_{73}	–8.94	–9.21	3.0	–11.20	25.3	–11.48	28.4
	F_{74}	11.99	12.20	1.8	10.28	–14.3	10.06	–16.1
Columns	F_{15}	–122.19	–122.34	0.1	–124.01	1.5	–124.01	1.5
	F_{16}	143.78	143.84	0.0	142.25	–1.1	142.20	–1.1
	F_{17}	–111.27	–111.05	–0.2	–108.87	–2.2	–109.16	–1.9
	F_{18}	129.37	129.27	–0.1	131.27	1.5	131.18	1.4
Cross-braces	F_{79}	9.89	9.81	–0.8	11.90	20.3	11.98	21.1
	F_{80}	–7.87	–7.69	–2.3	–5.47	–30.5	–5.54	–29.6
	F_{81}	–6.76	–7.26	7.4	–10.21	51.0	–9.79	44.8
	F_{82}	8.93	9.28	3.9	6.75	–24.4	6.75	–24.4

Table 6. Displacement values (u) of the node A

Displacement		Without flexible joints	With flexible joints					
			Cycle 1 Phase 1		Cycle 2 Phase 1		Cycle 5 Phase 1	
			u	$\frac{(4)-(3)}{(3)}100$	u	$\frac{(6)-(3)}{(3)}100$	u	$\frac{(8)-(3)}{(3)}100$
1	*2*	*3*	*4*	*5*	*6*	*7*	*8*	*9*
Node A	u_x [mm]	207.6	261.7	26.1	283.82	36.7	266.8	28.5
	u_y [mm]	8.103	10.333	27.5	10.205	25.9	9.009	11.2
	ϕ [°]	0.392	0.516	31.6	0.563	43.6	0.518	32.1

These results are used to compare the impact of joint flexibility on the values of forces in the columns and cross-braces, which were obtained after the first phase of the cycle: the first one (Column 4), the second one (Column 6) and the fifth one (Column 8), respectively.

As expected, the impact of joint flexibility on the values of the forces in columns is negligible and ranges from –2.2% (the force F_{17} in the second cycle) to 1.5% (the force F_{15} in the fifth cycle). It is visible only in the values of forces in cross braces connected to the column in nodes located directly under the flexible contact point and above the contact point. For example, in a compression cross brace located above the second contact point (Bar 81), the value of the axial force in the first cycle differs by 7.4%, in the second one by as much as 51%, and in the fifth one by 44.8%. Although these differences are large, they refer to low values of forces and could significantly affect the effort only of very slender cross braces.

Table 6 contains the values of displacements of the tower top (node A) in the same way as for the forces in Table 5.

The increase in the value of the horizontal displacement of the tower top, as compared to the solution without flexible nodes, is 26.1% after one cycle, 36.7% after two cycles, and 28.5% after five cycles. The value of the curb rotation angle in node A, which determines the serviceability limit state for radio antennas suspended in this place, increased in a similar way. After just one cycle, the value of this angle exceeded 0.5° to reach 0.56° after two cycles and 0.52° after five cycles. The angle of rotation of the radio link antenna $\alpha = 0.5°$ is considered to be the limit for good radio signal reception.

Based on these calculations, it is concluded that the flexibility of the column joints significantly affects the serviceability limit state of the tower, and in the case of slender cross braces can also determine their ultimate limit state.

CONCLUSIONS

The presented examples of lattice bar structures indicate that it is necessary to take into account the global flexibility of joints and the possibility of slip in these joints in the analysis. Flexible nodes may have a greater impact on the deformation of such structures than local bar arch imperfections. Similar influences are to be expected in roofs of single-storey industrial buildings, where, in addition to global imperfections, flexibility of the bracings rods connections may also be important (Zamorowski & Gremza, 2019).

The proposed formulas of the component method for estimating the rigidity of lap joints in terms of shift and rotation describe the behaviour of such joints during laboratory investigation quite well. They can be used in global structure analysis.

The presented node rigidity model, both for increasing loads and alternating loads, can be used in global structure analysis, provided that the model does not have horizontal straight lines as in the elastic-plastic model. The above reservation results from the fact that the secant node rigidity is defined as the internal

force to displacement ratio, which is determined from relation between force and displacement based on the internal force value.

The obtained results based on the lattice tower analysis indicate the need to undertake broader numerical and experimental research of bar structures with flexible nodes in terms of shift under alternating loads. Currently, this issue is being hardly recognized.

Monitoring of displacements and load capacity utilization of individual components of actual structure with flexible joints may be analyzed by means of residual magnetic field (RMF) and fiber Bragg glass (FBG) methods, described for example in the works (Juraszek, 2018a, 2018b, 2019a, 2019b, 2019c, 2020).

REFERENCES

Augustyn, J. & Śledziewski, E. (1976). *Awarie konstrukcji stalowych*. Warszawa: Arkady.

European Committee for Standardization [CEN] (2005). *Eurocode 3: Design of steel structures. Part 1-8: Design of joints* (EN 1993-1-8). Bruxelles: European Committee for Standardization.

Juraszek, J. (2018a). Hoisting machine brake linkage strain. *Archives of Mining Sciences*, *63* (3), 583–597. https://doi.org/10.24425/123676

Juraszek, J. (2018b). Strain and force measurement in wire guide. *Archives of Mining Sciences*, *63* (2), 321–334. https://doi.org/10.24425/122450

Juraszek, J. (2019a). Application of fiber optic FBG techniques in analysis of strain in engineering machines. *New Trends in Production Engineering*, *2* (1), 480–485. https://doi.org/10.2478/ntpe-2019-0051

Juraszek, J. (2019b). Residual magnetic field non-destructive testing of gantry cranes. *Materials*, *12* (4), 564. https://doi.org/doi: 10.3390/ma12040564

Juraszek, J. (2019c). Residual magnetic field for identification of damage in steel wire rope. *Archives of Mining Sciences*, *64* (1), 79–92. https://doi.org/10.24425/ams.2019.126273

Juraszek, J. (2020). Fiber Bragg sensors on strain analysis of power transmission lines. *Materials*, *13* (7), 1559. https://doi.org/10.3390/ma13071559

Karczewski, J.A., Wierzbicki, S. & Witkowski, J. (2003). Analiza numeryczna i badania doświadczalne sprężonych, nakładkowych połączeń śrubowych. In *VIII Konferencja Naukowa pt. Połączenia i węzły w konstrukcjach metalowych, Olsztyn–Łańsk, 16–19 października 2003* (pp. 255–264). Warszawa: Polska Izba Konstrukcji Stalowych.

Kishi, N. & Chen, W.F. (1990). Moment-rotation relation of semirigid connections with Angles. *Journal of Structural Engineering*, *116* (7), 1813–1834. https://doi.org/10.1061/(ASCE)0733-9445(1990)116:7(1813)

Wuwer, W. (2006). Podatne połączenia na sworznie jednostronne w prętowych konstrukcjach cienkościennych [Flexible joint with blind bolts in thin-walled bar construction] (habilitation thesis). *Zeszyty Naukowe. Budownictwo/Politechnika Śląska*, *105* (1710).

Zamorowski, J. (2013). *Przestrzenne konstrukcje prętowe z geometrycznymi imperfekcjami i podatnymi węzłami* [*Spatial bar structures with geometrics imperfections and flexible nodes*]. Gliwice: Wydawnictwo Politechniki Śląskiej.

Zamorowski, J. & Gremza, G. (2019). Modelling of roof bracings of single-storey industrial buildings. In F. Wald, M. Jandera (Eds.), *Stability and Ductility of Steel Structures 2019* (pp. 1309–1316). Leiden: CRC Press/Balkema. https://doi.org/10.1201/9780429320248

Zamorowski, J., Swierczyna, S. & Wuwer, W. (2011). Zastosowanie metody składnikowej wg PN-EN 1993-1-8 do oceny sztywności połączeń zakładkowych [Application of the component method according to PN-EN 1993-1-8 to assess the rigidity of lap joints]. *Inżynieria i Budownictwo*, *11*, 602–606.

NOŚNOŚĆ I STATECZNOŚĆ KONSTRUKCJI Z WĘZŁAMI PODATNYMI NA PRZESUW

STRESZCZENIE

W literaturze szeroko jest analizowane zagadnienie dystrybucji sił wewnętrznych w konstrukcjach prętowych w zależności od podatności węzłów na obrót. Rzadziej natomiast dyskutowane są wyniki badań takich konstrukcji z węzłami podatnymi na przesuw. W niniejszej pracy przedstawiono przykłady konstrukcji, w przypadku których podatność połączeń zakładkowych na przesuw decydowała o ich nośności i stateczności, a także stanach granicznych użytkowania. Opisano mało wyniosłą kopułę, przekrycie hali wystawowej

w Chorzowie, która w 2006 r. uległa zawaleniu, oraz wieżę telefonii komórkowej. Wykorzystano przy tym modele mechaniczne opisujące metodą składnikową sztywność różnych połączeń zakładkowych na obrót i przesuw oraz przedstawiono model matematyczny Kishiego i Chena, który służy do modelowania podatności połączeń zakładkowych przy obciążeniach przemiennych. Uzyskane wyniki wskazały, że w przypadku mało wyniosłej kopuły o awarii zadecydowały luzy w połączeniach. W przekryciu hali wystawowej w Chorzowie podatność połączeń doprowadziła do nadmiernego wytężenia niektórych płatwi kratowych, co mogło zainicjować katastrofę. Z kolei rzadko uwzględniana podatność połączeń przy projektowaniu wież telefonii komórkowych może doprowadzić do nadmiernego wychylenia krawężników wież, na których są zawieszone anteny radiolinii, a przez to może zakłócać transmisję danych. Na podstawie przeprowadzonej analizy można wnioskować o potrzebie uwzględniania wpływu podatnych węzłów nie tylko w konstrukcjach wrażliwych na deformację (np. mało wyniosła kopuła), ale też w konstrukcjach, w których decydujący może być stan graniczny użytkowania (np. wieże telefonii komórkowej).

Słowa kluczowe: podatność węzłów na przesuw, podatność połączeń zakładkowych na przesuw i obrót, modelowanie konstrukcji z podatnymi na przesuw węzłami